JMEPEG (2015) 24:3905–3911
DOI: 10.1007/s11665-015-1665-0

1059-9495/$19.00

Strengthening of Aluminum Alloy 2219 by Thermo-mechanical Treatment

Xifeng Li, Kun Lei, Peng Song, Xinqin Liu, Fei Zhang, Jianfei Li, and Jun Chen

(Submitted February 12, 2015; in revised form June 29, 2015; published online August 20, 2015)

Strengthening of aluminum alloy 2219 by thermo-mechanical treatment has been compared with artificial aging. Three simple deformation modes including pre-stretching, compression, and rolling have been used in thermo-mechanical treatment. The tensile strength, elongation, fracture feature, and precipitated phase have been investigated. The results show that the strengthening effect of thermo-mechanical treatment is better than the one of artificial aging. Especially, the yield strength significantly increases with a small decrease of elongation. When the specimen is pre-stretched to 8.0%, the yield strength reaches 385.0 MPa and increases by 22.2% in comparison to the one obtained in aging condition. The maximum tensile strength of 472.4 MPa is achieved with 4.0% thickness reduction by compression. The fracture morphology reveals locally ductile and brittle failure mechanism, while the coarse second-phase particles distribute on the fracture surface. The intermediate phases θ'' or θ' orthogonally precipitate in the matrix after thermo-mechanical treatment. As compared to artificial aging, the cold plastic deformation increases distribution homogeneity and the volume fraction of θ'' or θ' precipitates. These result in a better strengthening effect.

Keywords aluminum alloy 2219, precipitate, strengthening, thermo-mechanical treatment

1. Introduction

Aluminum alloys are attracting attentions from researchers, engineers, and designers as promising structural materials for aerospace and automotive industries. Their properties can be improved by specific heat treatment methods. This process usually includes two typical stages: solution heat treatment and artificial aging. In solution heat treatment, the alloys are heated up to a specific temperature at which all the alloying elements are in solution status. After that, the material is further heated to a temperature above room temperature and held for a period of time called as "artificial aging (Ref 1, 2)." Compared with natural aging, the precipitation is accelerated, and the strength is further increased. Additionally, thermo-mechanical treatment process, including three main procedures of solution-quenching, plastic deformation, and artificial aging, also has been used to improve the mechanical properties of aluminum alloys.

Aluminum alloy 2219 is an Al-Cu binary alloy. It is widely used in cryogenic tanks, fuselage, and shells for space vehicles due to good toughness, high strength, and favorable weldability characteristics coupled with higher usage temperature (Ref 3). Some researchers have studied the mechanical properties and microstructural variation under different conditions. Qu et al. discussed the influences of temperature and heat treatment status on the fracture toughness of aluminum alloy 2219. The experimental results showed that the ductile fracture values significantly increase with a decrease of temperature from 15 to −182 °C (Ref 4). Zhang et al. examined the effect of initial microstructure on the hot compression deformation behavior of aluminum alloy 2219. Compared with the newly as-homogenized microstructure, the as-aged state was featured by a larger volume fraction of second-phase particles, whereas the as-quenched microstructure was featured by a higher dissolved Si concentration in the α-Al matrix. The difference in the activation energy for these three states was attributed to the different contents of Si in α-Al solid solution (Ref 5).

The selection and application of aluminum alloy 2219 for structural components are severely constrained by insufficient tensile strength and ductility. The strengthening of aluminum alloy 2219 by artificial aging has been widely investigated. Rosen et al. investigated the age-hardening process in aluminum alloy 2219 by means of dynamic measurements of sound wave velocity, ultrasonic attenuation, and hardness. These properties were changed as a function of aging time at constant temperatures, which were related to the formation of θ'' and θ' precipitates (Ref 6). Ber proposed step-aging regimes for aluminum alloy 2219 with first low-temperature stage and second high-temperature stage. The tensile properties, corrosion resistance, and resource characteristics of semi-products treated by standard and accelerated regimes were compared (Ref 7). Shanmugasundaram et al. reported the precipitation hardening of aluminum alloy 2219 subjected to cryorolling, low-temperature annealing, and aging treatments. Ultrafine-grained microstructures with improved tensile strength (540MPa) and good ductility (11% tensile elongation) were obtained under optimal processing condition (Ref 8). However, this method has some disadvantages, such as the dangerous condition in handling a workpiece under liquid nitrogen temperature, the limited strain for each pass and high cost. Rafi Raza et al. strengthened aluminum alloy 2219 by mechanical working and heat treatment. The maximum ulti-

Xifeng Li and **Jun Chen**, Department of Plasticity Technology, Shanghai Jiao Tong University, Shanghai 200030, People's Republic of China; **Kun Lei, Peng Song,** and **Xinqin Liu**, Institute of Aerospace Special Material and Technology, Beijing 100074, People's Republic of China; **Fei Zhang**, AVIC Xi'an Aircraft Industry (Group) Company Ltd., Xi'an 710089, People's Republic of China; and **Jianfei Li**, AVIC Chengdu Aircraft Industry (Group) Company Ltd., Chengdu 610091, People's Republic of China. Contact e-mail: jun_chen@sjtu.edu.cn.

mate tensile strength of 410.9 MPa was achieved by aging at 210 °C for 4 h (Ref 9).

The thermo-mechanical treatment process can effectively change the microstructure and mechanical properties of aluminum alloys (Ref 10-13). An et al. investigated the effect of pre-deformation on the microstructure and mechanical properties of aluminum alloy 2219 sheet by thermo-mechanical treatment process. A pre-deformation procedure was introduced before the traditional thermo-mechanical treatment process by developing a special experimental setup to produce uniaxial tensile specimens with different plastic deformation values. The maximum tensile strength of about 388 MPa was obtained with the pre-deformation of about 2% (Ref 14). However, the experimental method was relatively complicated. Additionally, the obtained maximum yield and tensile strength were lower as compared to artificial aging. Overall, the effect of thermo-mechanical treatment on the mechanical properties of aluminum alloy 2219 was less reported. Further studies on the strengthening of aluminum alloy 2219 by thermo-mechanical treatment process are very necessary.

Actually, the components of aluminum alloy 2219 produced by warm forming have relatively low strength, which severely restricts the application. The significance of aluminum alloy 2219 used in aerospace field impels to investigate the strengthening methods and intrinsic microstructure mechanisms. In the presented work, the effect of thermo-mechanical treatment on the mechanical properties of aluminum alloy 2219 compared with artificial aging is investigated. Three simple deformation modes including pre-stretching, compression, and rolling are adopted in thermo-mechanical treatment. The microstructural mechanism governing the tensile behavior of the alloy is discussed as well.

2. Experimental Procedures

The commercial aluminum alloy 2219 sheet with thickness of 10 mm in this study was provided in the annealed state. The specimen with 30 mm × 180 mm is cut along the rolling direction. The chemical compositions are listed in Table 1. The specimens were solution treated at 535 °C for 50 min in Nabertherm low-temperature furnace with control accuracy as ±2 °C. Then, the specimens were quenched in water at room temperature. For thermo-mechanical treatment process, the quenched sheets along initial rolling direction were performed by pre-stretching, compression, and rolling at room temperature, respectively. Different tensile deformation amount and thickness reductions were also compared. Tensile elongation was 2.0, 5.0, 8.0, and 10.0%, while the sheets were compressed and rolled by the thickness reductions of 3.0-7.0, and 2.0-8.5%, respectively. Finally, the deformed sheets were artificially aged at 160 °C for 24 h. The detailed procedure of thermo-mechanical treatment process is shown in Fig. 1. For comparison with thermo-mechanical treatment, the quenched sheets without deformation were also artificially aged at 160 °C for 24 h. According to Chinese standards, the tensile specimens were prepared from the treated sheets with 12.5 mm × 50 mm gage as shown in Fig. 2. The gage size is same as pre-stretching specimen. Uniaxial tensile tests were conducted at an initial strain rate of 1×10^{-3} s^{-1} and under a constant cross-head speed. All tests were performed at least three times in order to ensure the repeatability and reproducibility of the results.

The fracture surface of tensile specimens was examined by a JSM7600F scanning electron microscope (SEM) to study the microscopic fracture mode. The precipitation phases were observed by a JEM2100 type transmission electron microscope (TEM) operating at an accelerated voltage of 200kV. All of the TEM specimens were prepared using twin-jet polishing with a solution of 20% nitric acid and 80% methanol.

3. Results and Discussion

Figure 3 shows the tensile stress-strain curves of 2219 aluminum alloy sheet under different conditions. The flow stress of the thermo-mechanical treatment samples exceeds that

Table 1 Chemical compositions of 2219 aluminum alloy (wt.%)

Cu	Mn	Si	Zr	Fe	Ti	Zn	Mg	Al
6.44	0.35	0.17	0.11	0.09	0.04	0.02	0.01	Balance

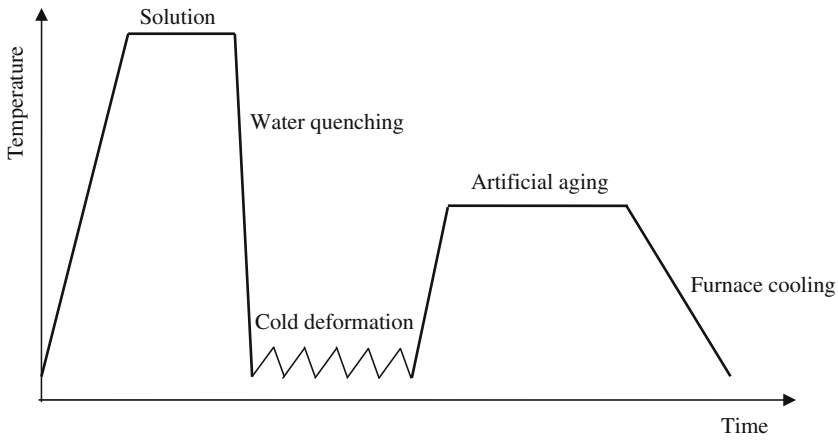

Fig. 1 Schematic diagram of thermo-mechanical treatment process

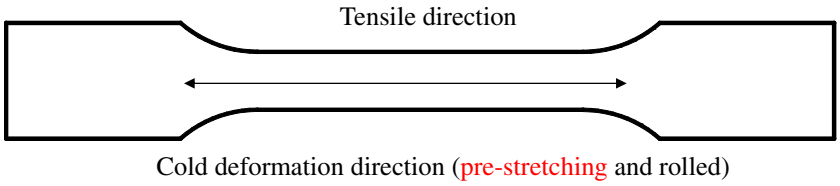

Fig. 2 Schematic diagram of tensile specimen after thermo-mechanical treatment

Table 2 Strengthening effect of aluminum alloy 2219 sheets under different conditions

Processing condition						Strengthened effect compared with aging	
Deformation mode	Deformation value, %	Heat treatment	Yield strength, $\sigma_{0.2}$, MPa	Ultimate tensile strength, σ_b, MPa	Elongation, %	$\Delta\sigma_{0.2}$, MPa	$\Delta\sigma_b$, MPa
		As-received	91.6	189.1	28.0	···	···
		Quenched	151.9	344.3	23.7	···	···
	0	Aged at 160 °C for 24 h	315.0	458.7	15.4	···	···
Tension	2.0		342.5	460.8	14.7	27.5	2.1
	5.0		374.8	464.5	14.7	59.8	5.8
	8.0		385.0	471.8	13.9	70.0	13.1
	10.0		380.4	468.7	13.0	65.4	10.0
Compression	3.0		355.0	464.3	14.0	40.0	5.6
	4.0		360.0	472.4	14.0	45.0	13.7
	7.0		375.0	468.9	12.6	60.0	10.2
Rolling	2.0		352.5	468.7	15.1	37.5	10.0
	5.0		365.0	465.2	14.1	50.0	6.5
	8.5		377.5	467.9	14.4	62.5	9.2

Table 3 Strain-hardening exponent (n), the ratio of yield strength and ultimate tensile strength ($\sigma_{0.2}/\sigma_b$), and static toughness (U) of aluminum alloy 2219 under different conditions

				Thermo-mechanical treatment		
	As-received	Quenched	Aging	5.0% tension	4.0% compression	5.0% rolling
n	0.29	0.43	0.33	0.23	0.27	0.25
$\sigma_{0.2}/\sigma_b$	0.48	0.44	0.69	0.81	0.76	0.78
U (MJ/m^3)	46.5	65.9	58.4	59.9	57.1	57.4

of the artificial aging ones. Additionally, the tensile curves of thermo-mechanical treatment indicate a little difference in strength and elongation. The mean values of the mechanical properties are summarized in Table 2. The yield strength and ultimate tensile strength are greatly improved and the elongation is slightly decreased for all the thermo-mechanical treatment samples compared with that of the aging condition. The maximum tensile strength reaches 472.4 MPa when the specimen is compressed with 4.0% thickness reduction. Obviously, the strengthening result by thermo-mechanical treatment is better than that of artificial aging with different temperature and time reported by others (Ref 7, 9). The strength change is attributed to the volume fraction and size of the precipitates. The precipitates with higher volume fraction and finer size are obtained in the study. Consequently, the yield strength and ultimate tensile strength can be greatly improved. The yield strength almost increases with increasing deformation amount, while the peak value of ultimate tensile strength appears at a certain deformation amount in different deformation modes. Specifically, the ultimate tensile strength initially increases with deformation amount, reaches a maximum value, and then slightly decreases. Moreover, the increase of yield strength is much greater than that of ultimate tensile strength. When the specimen is pre-stretched to 8.0%, the yield strength value reaches 385.0 MPa. The yield strength and ultimate tensile strength are increased by 22.2 and 2.9% in comparison to aging condition. Similarly, the yield strength and ultimate tensile strength are increased by 14.3 and 3.0% when the specimen is compressed to 4.0% thickness reduction. The above results demonstrate that the thermo-mechanical treatment process can efficiently improve the strength with sacrificing small elongation compared with artificial aging.

The strain-hardening exponent (n) listed in Table 3 was calculated according to the Eq 1 fitting the true stress-strain curves of aluminum alloy 2219 in Fig. 3(b) (Ref 15).

$$\sigma = K\varepsilon^n. \quad \text{(Eq 1)}$$

In the power-hardening mode, σ is the flow stress, K is the hardening coefficient, and ε is true strain. K value is also obtained by fitting the curves in Fig. 3(b) by Eq 1. Actually, n value is almost inverse to the ratio of yield strength and ultimate tensile strength ($\sigma_{0.2}/\sigma_b$). Because the increased

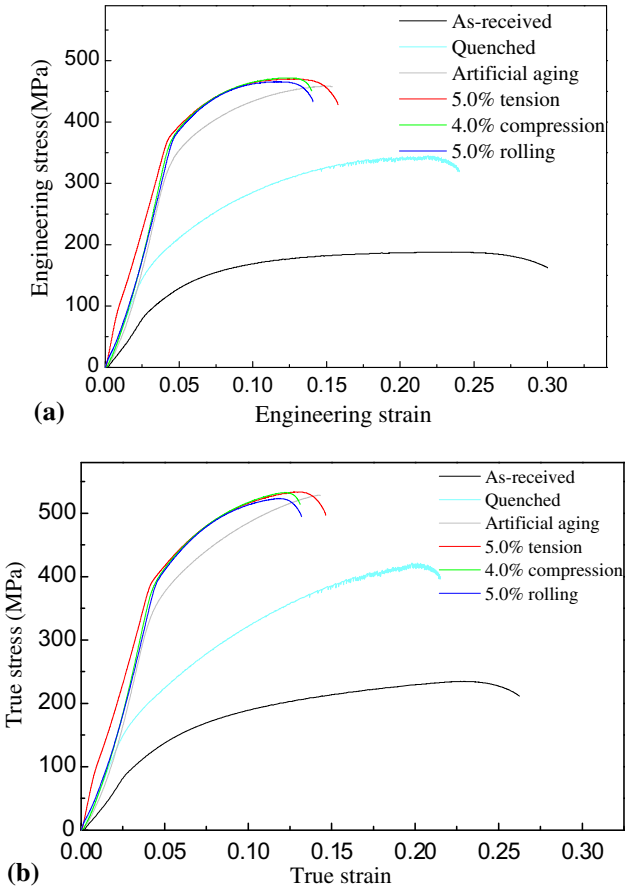

Fig. 3 Tensile stress-strain curves of aluminum alloy 2219 sheets under different conditions: (a) engineering strain-stress curves, (b) true strain-stress curves (Color figure online)

amount of yield strength is more obvious than that of ultimate tensile strength, n value of aluminum alloy 2219 by thermo-mechanical treatment is lower compared with quenched and aging state. The strain-hardening exponent n is about 0.23-0.27 after thermo-mechanical treatment.

Static toughness (U) represents good coordination of strength and plasticity, which can be calculated by Eq 2 (Ref 16).

$$U = \int_0^{\varepsilon_f} \sigma d\varepsilon, \qquad \text{(Eq 2)}$$

where σ is the flow stress and ε_f is the total strain at fracture. Combining Eq 1 with Eq 2, the static toughness U can be expressed by Eq 3.

$$U = \frac{K}{n+1}\varepsilon^{n+1}\Big|_0^{\varepsilon_f} \qquad \text{(Eq 3)}$$

According to Eq 3, the static toughness values of aluminum alloy 2219 at different conditions are also listed in Table 3. Obviously, aluminum alloy 2219 in the quenched state has the maximum static toughness. It can be explained that the ultimate tensile strength of the quenched state is much higher than that of the as-received state with 15.4% elongation loss. The static toughness U of aluminum alloy 2219 is almost constant of 57-60 MJ/m^3 after thermo-mechanical treatment, which is less than 2.6% deviation compared with that of the aged state. The strength of aluminum alloy 2219 can be obviously improved,

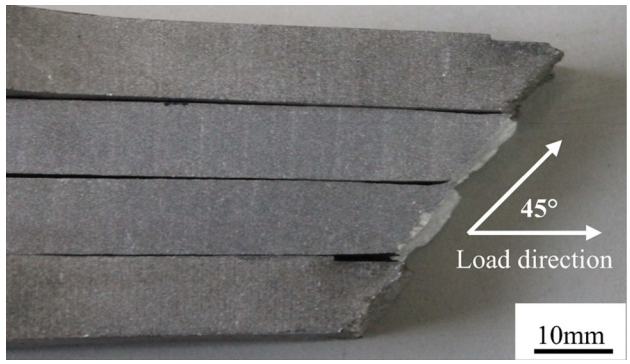

Fig. 4 Fracture specimens of aluminum alloy 2219 after artificial aging and thermo-mechanical treatment

while the static toughness is nearly the same as the aged state. Therefore, the thermo-mechanical treatment process is a promising method in adjusting the comprehensive mechanical properties among strength, elongation, and static toughness of aluminum alloy 2219.

Figure 4 shows the fracture specimens of aluminum alloy 2219 after artificial aging and thermo-mechanical treatment. From the macroscopic view, the fracture surfaces reveal little difference in overall fracture morphology. Obviously, the angle between fracture surface and load direction is about 45°, which indicates shear fracture mode. This result is consistent with that found by Fang et al. but inconsistent with that reported by Srivatsan et al. (Ref 17, 18). The shear facture surface is close to the maximum shear stress plane for aluminum alloy 2219 subjected to artificial aging and thermo-mechanical treatment. This indicates that the fracture mode should be mainly controlled by the maximum shear stress.

At the microscopic level, the typical fracture morphologies of the samples under different conditions are shown in Fig. 5. Compared with the samples treated by thermo-mechanical treatment, many deeper dimples distribute on the fracture surface after artificial aging in Fig. 5(a), which indicates better ductility. Figure 5 (b) shows a few shallow dimples and microscopic voids that distribute on the fracture surface after thermo-mechanical treatment. They result from the presence of the second-phase particles. Figure 5(c) shows higher resolution observation corresponding to circle region in Fig. 5(b). The coarse second-phase particles with about 2.5 μm should be Al_3Zr (Ref 18). As shown in Fig. 5(e), the microscopic voids, shallow dimples, and secondary microscopic cracks appear on the fracture surface. The formation of microscopic voids and secondary cracks easily results in the elongation reduction. When the elastic energy of the second-phase particle in the matrix is higher than the surface energy of the newly formed void surface, the void nucleates at the particle. Furthermore, the halves of the voids are the shallow dimples. The coalescence of microscopic voids leads to secondary microscopic cracks. The secondary microscopic cracks easily propagate along the grain boundaries and eventually result in intergranular type fracture (Ref 18). Therefore, the fracture features overall reveal locally ductile and brittle failure.

The second-phase particles disengage from the grain boundaries, forming microvoids which grow and coalesce continuously to microscopic cracks, leading to final facture. For aluminum alloy 2219, the interaction between the high resolved shear stress and the shearable second-phase particles in the

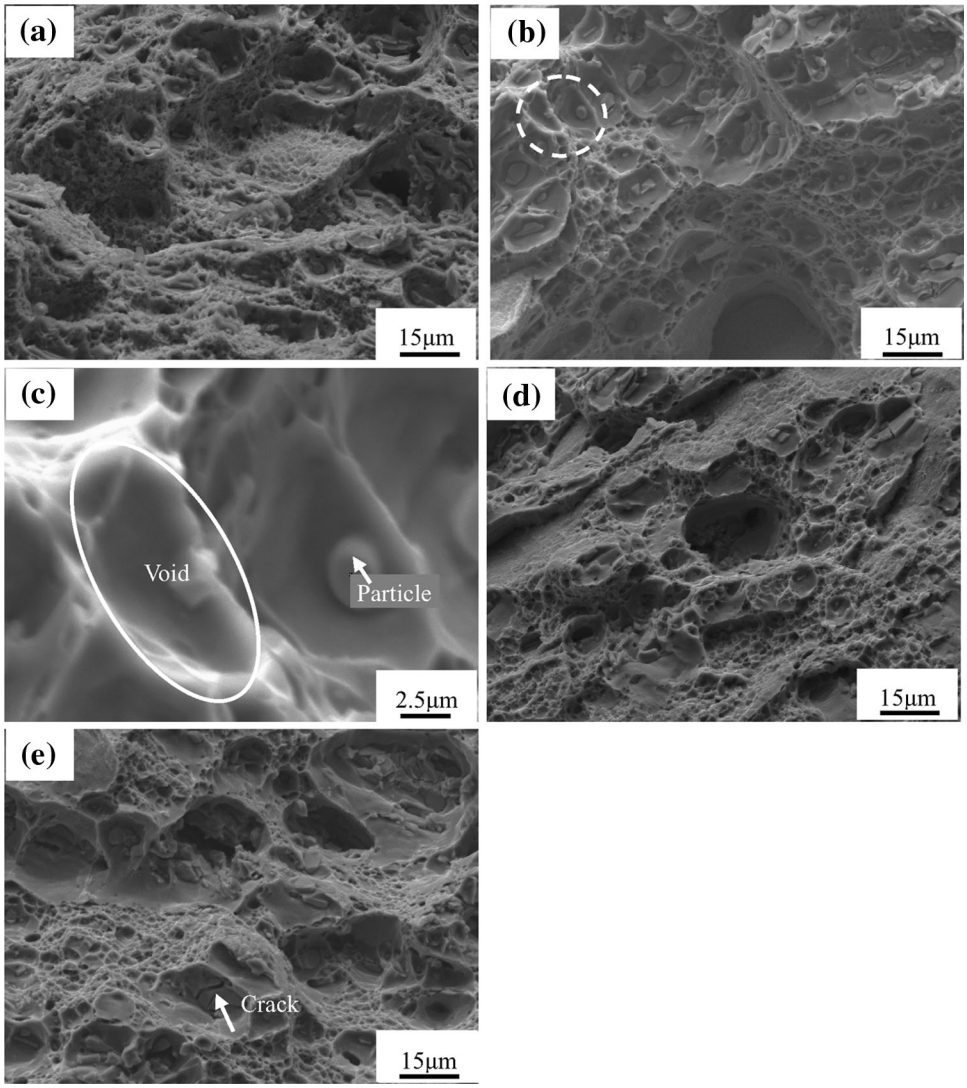

Fig. 5 SEM fracture morphologies of aluminum alloy 2219 under different conditions: (a) artificial aging, (b) 5.0% pre-stretching elongation, (c) enlarged image corresponding to circle region in Fig. 3(b) and (d) 4.0% thickness reduction by compression, and (e) 5.0% thickness reduction by rolling

matrix leads to the occurrence of transcrystalline localization. The microvoids are difficult to grow and aggregate due to the effect of these particles at fracture zones. Thus, the shear fracture becomes more predominant under tensile deformation.

The TEM microstructure under different conditions shows needle-like precipitates in Fig. 6. Figure 6(a) reveals that the phases θ'' or θ' only precipitate along one direction when the specimens are treated by artificial aging. Nevertheless, the precipitated phases are orthogonally dispersed in the matrix when the specimens are treated by thermo-mechanical treatment shown in Fig. 6(b)-(d). The similar precipitated morphology was found by Shanmugasundaram et al. (Ref 8). Furthermore, in comparison with that treated by artificial aging, the size and volume fraction of the precipitated phases θ'' or θ' are obviously larger in the samples treated by thermo-mechanical treatment. The precipitation sequence during aging of Al-Cu alloys is G.P. zones $\rightarrow$ θ'' $\rightarrow$ θ' $\rightarrow$ θ. The observed precipitates are intermediate phases θ" or θ' which are very coherent with the matrix and can improve the strength (Ref 8, 19). In aluminum alloy 2219, the precipitated strengthening plays a key role in aging treatment. Compared with G.P. zones, the intermediate phase preferentially nucleates at grain boundaries and dislocation pile-ups due to the required high nucleation energy. The cold plastic deformation is performed after quenching in the specimens. Then, the dislocation density, nucleation sites, nucleation, and growth rate of θ'' or θ' phases are increased. Therefore, the precipitated phases orthogonally grow fast. The distribution homogeneity and volume fraction of the precipitated phases in the matrix can be improved. The precipitates can pin the dislocations and inhibit the movement of the dislocations during tensile deformation. This makes further deformation in the specimens difficult and directly strengthened. Consequently, compared with artificial aging, the thermo-mechanical treatment has a better strengthening effect, which is also verified in Fig. 3 and Table 2. The experimental data indicate that there is an optimum deformation value under pre-stretching, compression, and rolling modes. Under the optimal deformation value, there is the most uniform distribution and the highest dispersion degree of the θ″ or θ′ precipitates. Thus, the highest ultimate tensile strength exists.

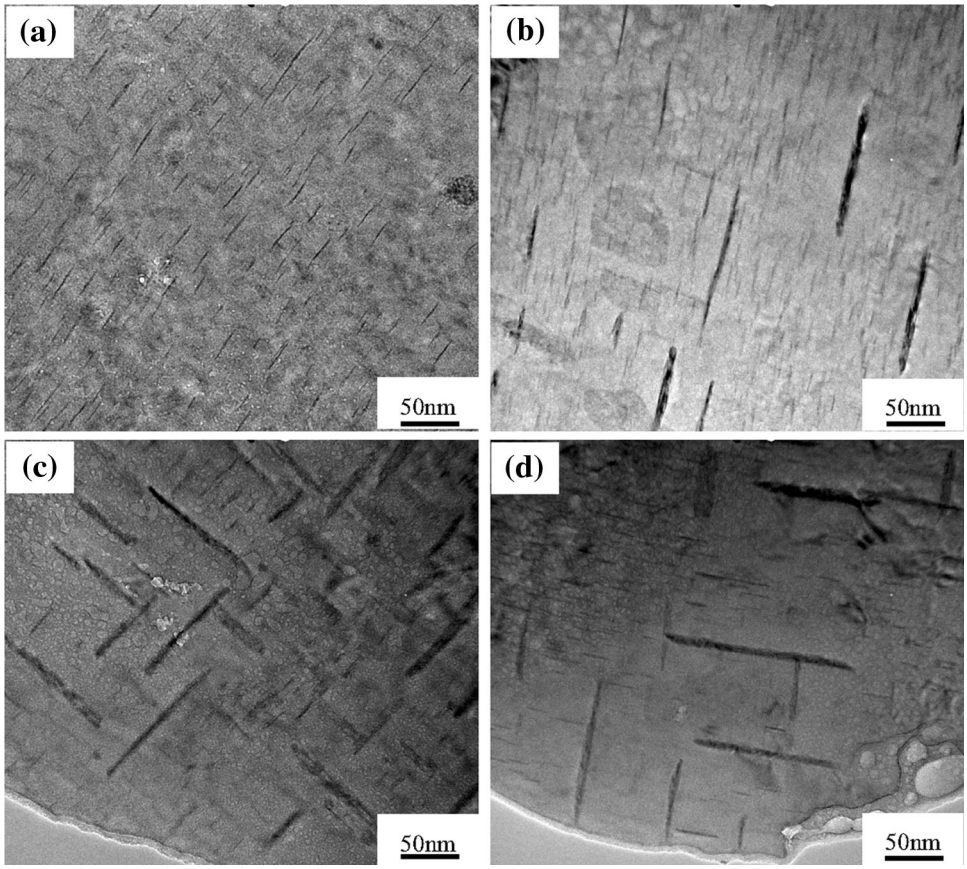

Fig. 6 TEM micrographs of aluminum alloy 2219 under different conditions: (a) artificial aging without deformation; (b) 5.0% pre-stretching elongation; (c) 4.0% thickness reduction by compression; and (d) 5.0% thickness reduction by rolling

Additionally, the yield strength and ultimate tensile strength obtained in this study are far higher than those in the Ref 14. This perhaps results from much finer precipitated phase θ'' or θ'. The average size of θ'' or θ' precipitates in this study is approximately 100 nm. However, the θ'' or θ' phases with about 150 nm were precipitated (Ref 14). According to Orowan age-strengthening model (Ref 20), the average radius of the precipitates plays an important role in strengthening effect. It has a positive effect on the strength increase with the decrease of the precipitate size. Moreover, the finer precipitated phase can easily inhabit the crack initiation and propagation. It accounts for small elongation decrease by thermo-mechanical treatment as well.

4. Conclusions

The thermo-mechanical treatment process of aluminum alloy 2219 by three simple deformation modes including pre-stretching, compression, and rolling is comprehensively studied. Strengthening effect by thermo-mechanical treatment is compared with artificial aging. Aluminum alloy 2219 with high strength and good ductility is obtained by thermo-mechanical treatment. The following conclusions can be drawn:

(1) The thermo-mechanical treatment has a better strengthening effect compared with artificial aging in aluminum alloy 2219, especially for improving yield strength. When the specimen is pre-stretched to 8.0%, YS reaches 385.0 MPa and is increased by 22.2% in comparison to the aged state. This method can effectively improve the comprehensive mechanical properties among strength, elongation, and static toughness.

(2) The second-phase particles distributed on the fracture surface restrict microvoids to grow and aggregate. Aluminum alloy 2219 shows shear fracture mode after artificial aging and thermo-mechanical treatment. The fracture morphology demonstrates locally ductile and brittle failure mechanism.

(3) The intermediate phases θ'' or θ' orthogonally precipitate in the matrix after thermo-mechanical treatment. Compared with artificial aging, the cold plastic deformation after quenching obviously increases distribution homogeneity and volume fraction of θ'' or θ' phase and leads to a better strengthening effect.

(4) The strength of aluminum alloy 2219 can reach 470 MPa with good ductility after thermo-mechanical treatment. This is beneficial to expand the application aluminum alloy 2219 in aerospace field.

References

1. K.S. Kumar, S.A. Brown, and J.R. Pickens, Microstructural Evolution During Aging of an Al-Cu-Li-Ag-Mg-Zr Alloy, *Acta Mater.*, 1996, **44**, p 1899–1915
2. H. Demir and S. Gündüz, The Effects of Aging on Machinability of 6061 Aluminum Alloy, *Mater. Des.*, 2009, **30**, p 1480–1483

3. R. Kaibyshev, I. Kazakulov, D. Gromov, F. Musin, D.R. Lesuer, and T.G. Nieh, Superplasticity in a 2219 Aluminum Alloy, *Scr. Mater.*, 2001, **44**, p 2411–2417
4. W.Q. Qu, M.Y. Song, J.S. Yao, and H.Y. Zhao, Effect of Temperature and Heat Treatment Status on the Ductile Fracture Toughness of 2219 Aluminum Alloy, *Mater. Sci. Forum*, 2011, **689**, p 302–307
5. J. Zhang, B.Q. Chen, and B.X. Zhang, Effect of Initial Microstructure on the Hot Compression Deformation Behavior of a 2219 Aluminum Alloy, *Mater. Des.*, 2012, **34**, p 15–21
6. M. Rosen, E. Horowitz, S. Fick, R.C. Reno, and R. Mehrabian, An Investigation of the Precipitation-hardening Process in Aluminum Alloy 2219 by Means of Sound Wave Velocity and Ultrasonic Attenuation, *Mater. Sci. Eng.*, 1982, **53**, p 163–177
7. L.B. Ber, Accelerated Artificial Ageing Regimes of Commercial Aluminum Alloys. II: Al-Cu, Al-Zn-Mg-(Cu), Al-Mg-Si-(Cu) Alloys, *Mater. Sci. Eng. A*, 2000, **280**, p 91–96
8. T. Shanmugasundaram, B.S. Murty, and V. Subramanya Sarma, Development of Ultrafine Grained High Strength Al-Cu Alloy by Cryorolling, *Scr. Mater.*, 2006, **54**, p 2013–2017
9. M. Rafi Raza, F. Ahmad, N. Ikram, R. Ahmad, and A. Salam, Development and Strengthening of 2219 Aluminum Alloy by Mechanical Working and Heat Treatment, *J. Appl. Sci.*, 2011, **11**, p 1857–1861
10. Z.M. El-Baradie and M. El-Sayed, Effect of Double Thermomechanical Treatments on the Properties of 7075 Al Alloy, *J. Mater. Proc. Technol.*, 1996, **62**, p 76–80
11. M. Song, Y.H. He, D.H. Xiao, and B.Y. Huang, Effect of Thermomechanical Treatment on the Mechanical Properties of an Al-Cu-Mg Alloy, *Mater. Des.*, 2009, **30**, p 857–861
12. T.S. Parel, S.C. Wang, and M.J. Starink, Hardening of an Al-Cu-Mg Alloy Containing Types I, and II, S Phase Precipitates, *Mater. Des.*, 2010, **31**, p S2–S5
13. Y.J. Huang, Z.G. Chen, and Z.Q. Zheng, A Conventional Thermomechanical Process of Al-Cu-Mg Alloy for Increasing Ductility While Maintaining High Strength, *Scr. Mater.*, 2011, **64**, p 382–385
14. L.H. An, Y. Cai, W. Liu, S.J. Yuan, S.Q. Zhu, and F.C. Meng, Effect of Pre-deformation on Microstructure and Mechanical Properties of 2219 Aluminum Alloy Sheet by Thermomechanical Treatment, *Trans. Nonferrous Met. Soc. China*, 2012, **22**, p S370–S375
15. E.S. Puchi and M.H. Staia, Mechanical Behavior of Aluminum Deformed Under Hot-Working Conditions, *Metall. Mater. Trans. A*, 1995, **26**, p 2895–2910
16. W.D. Callister, *Fundamentals of Materials Science and Engineering*, Wiley, New York, 2001
17. D.R. Fang, Z.F. Zhang, S.D. Wu, C.X. Huang, H. Zhang, N.Q. Zhao, and J.J. Li, Effect of Equal Channel Angular Pressing on Tensile Properties and Fracture Modes of Casting Al-Cu Alloys, *Mater. Sci. Eng. A*, 2006, **426**, p 305–313
18. T.S. Srivatsan, S. Vasudevan, L. Park, and R.J. Lederich, The Quasi-static Deformation and Final Fracture Behavior of Aluminum Alloy 2219, *Mater. Sci. Eng. A*, 2008, **497**, p 270–277
19. Z. Cvijović, G. Radenković, V. Maksimović, and B. Dimčić, Application of ANOVA Method to Precipitation Behaviour Studies, *Mater. Sci. Eng. A*, 2005, **397**, p 195–203
20. S.-I. Hahn and S.J. Hwang, Estimate of the Hall-Petch and Orowan Effects in the Nanocrystalline Cu with Al_2O_3 Dispersoid, *J. Alloy Compd.*, 2009, **483**, p 207–208